

AD/A-003 473

APPLICATION OF RAY THEORY TO LOW  
FREQUENCY PROPAGATION

Henry Weinberg

Naval Underwater Systems Center  
New London, Connecticut

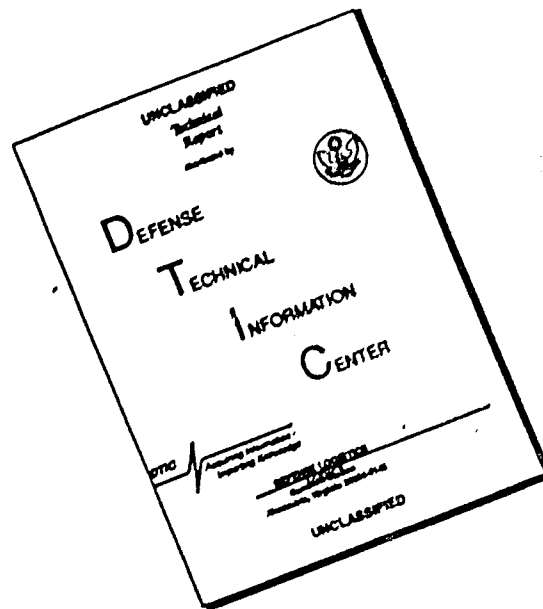
18 December 1974

DISTRIBUTED BY:

**NTIS**

National Technical Information Service  
U. S. DEPARTMENT OF COMMERCE

# DISCLAIMER NOTICE



THIS DOCUMENT IS BEST QUALITY AVAILABLE. THE COPY FURNISHED TO DTIC CONTAINED A SIGNIFICANT NUMBER OF PAGES WHICH DO NOT REPRODUCE LEGIBLY.

UNCLASSIFIED

SECURITY CLASSIFICATION OF THIS PAGE (When Data Entered)

REPORT DOCUMENTATION PAGE		READ INSTRUCTIONS BEFORE COMPLETING FORM
1. REPORT NUMBER TR 4867	2. GOVT ACCESSION NO.	3. RECIPIENT'S CATALOG NUMBER <b>AD/A-003473</b>
4. TITLE (and Subtitle) APPLICATION OF RAY THEORY TO LOW FREQUENCY PROPAGATION		5. TYPE OF REPORT & PERIOD COVERED
7. AUTHOR(s) Henry Weinberg		6. PERFORMING ORG. REPORT NUMBER
9. PERFORMING ORGANIZATION NAME AND ADDRESS Naval Underwater Systems Center New London Laboratory New London, Connecticut 06320		10. PROGRAM ELEMENT, PROJECT, TASK AREA & WORK UNIT NUMBERS A-654-03 ZR 000-01-01 61152N
11. CONTROLLING OFFICE NAME AND ADDRESS Naval Material Command Washington, D. C. 20362		12. REPORT DATE 18 December 1974
14. MONITORING AGENCY NAME & ADDRESS (if different from Controlling Office)		13. NUMBER OF PAGES 34
		15. SECURITY CLASS. (of this report) UNCLASSIFIED
16. DISTRIBUTION STATEMENT (of this Report) Approved for public release; distribution unlimited.		15a. DECLASSIFICATION/DOWNGRADING SCHEDULE
17. DISTRIBUTION STATEMENT (of the abstract entered in Block 20, if different from Report)		
18. SUPPLEMENTARY NOTES NATIONAL TECHNICAL INFORMATION SERVICE		
19. KEY WORDS (Continue on reverse side if necessary and identify by block number) Low Frequency Propagation Ray Theory CONGRATS V Caustics		
20. ABSTRACT (Continue on reverse side if necessary and identify by block number) The development of ray tracing techniques is reviewed, and then the effects of various sound-speed representations on the computed value of propagation loss are discussed. Since modified ray theories designed to treat caustics lose their effectiveness at the lower acoustic frequencies, an alternative approach for the horizontally stratified case is proposed. For oceans that are nearly horizontally stratified, the method of horizontal rays is applicable. Computed predictions are compared with measured data.		

DD FORM 1473  
1 JAN 73

EDITION OF 1 NOV 65 IS OBSOLETE  
S/N 0102-014-6601

UNCLASSIFIED

SECURITY CLASSIFICATION OF THIS PAGE (When Data Entered)

## TABLE OF CONTENTS

	Page
LIST OF ILLUSTRATIONS . . . . .	ii
INTRODUCTION . . . . .	1
RAY TRACING EQUATIONS . . . . .	1
SOUND SPEED REPRESENTATIONS . . . . .	3
ASYMPTOTIC TREATMENT OF CAUSTICS . . . . .	7
LOW FREQUENCY PROPAGATION IN HORIZONTALLY STRATIFIED OCEANS . . . . .	12
A COMPARISON OF PROPAGATION MODELS . . . . .	15
HORIZONTAL RAY THEORY FOR NEARLY HORIZONTALLY STRATIFIED OCEANS . . . . .	20
SUMMARY . . . . .	27
REFERENCES . . . . .	29

## LIST OF ILLUSTRATIONS

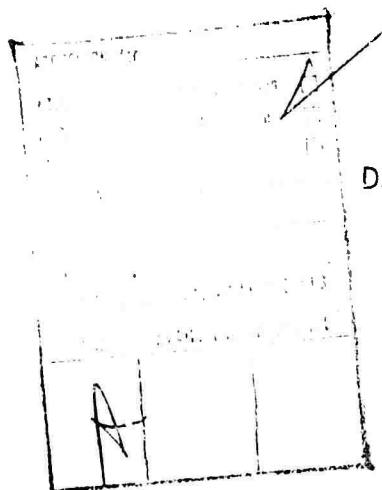
Figure		Page
1	Comparison of Sound Speed Representations and Gradients . .	4
2	Comparison of Ray Diagrams for an Axial Source . . . . .	5
3	Comparison of 1-kHz Propagation Losses for a 40-m Receiver Depth . . . . .	6
4	Sound Speed and Gradient Studied by Pedersen and Gordon . .	7
5	Ray Diagram for a 1-kyd Source Depth Computed by Using the Sound Speed of Figure 4 . . . . .	8
6	Comparison of 2-kHz Propagation Losses for a 0.8-kyd Receiver Depth Computed According to Classical and Modified Ray Theories . . . . .	9
7	Propagation Loss for a 0.8-kyd Receiver Depth Computed More Accurately Than That for Classical or Modified Ray Theories . . . . .	10
8	Classical Rays Used to Compute a Uniform Asymptotic Solution at a Caustic . . . . .	11
9	The Principal Ray Types . . . . .	13
10	Low Frequency Surface Duct Propagation for a Pacific Sound Speed Profile . . . . .	16
11	Low Frequency Convergence Zone Propagation for a Pacific Sound Speed Profile . . . . .	18
12	Contour of Sound Speed Along the Meridian 157° 50'W . . . .	22
13	Propagation Loss versus Range for a 2500-ft Receiver Depth, a 500-ft Source Depth, and a 31-Hz Frequency . . . . .	23
14	Sound Speed-Depth Profile at 27° 30'N, 157° 50'W and the Corresponding First Four Modes for a 31-kHz Frequency . .	24
15	Sound Speed-Depth Profile at 50° 0'N, 157° 50'W and the Corresponding First Four Modes for a 31-Hz Frequency . .	25
16	Propagation Loss versus Range for a 10,800-ft Receiver Depth, a 500-ft Source Depth, and a 31-Hz Frequency . . .	26

## PREFACE

This report was prepared under Project No. A-654-03, "Analysis of Acoustic Propagation in Ocean Environments," Principal Investigator, L. A. Stallworth (Code PA41), and Navy Subproject and Element No. ZR 000-01-01 61152N, Program Manager, T. A. Kleback, Naval Material Command (MAT 03521).

The Technical Reviewer for this report was J. S. Cohen (Code PA41).

REVIEWED AND APPROVED: 18 December 1974



*R. M. Dunlap*

R. M. Dunlap  
Director, Plans and Analysis

The author of this report is located at the New London Laboratory, Naval Underwater Systems Center, New London, Connecticut 06320.

## APPLICATION OF RAY THEORY TO LOW FREQUENCY PROPAGATION

### INTRODUCTION

It is often said that ray theory is not applicable to low frequency propagation in the ocean. The purpose of this report is to demonstrate that this is not the case. If the word "ray" is allowed a more general meaning than that used in the classical sense, then ray tracing is indeed a useful means of modeling low frequency propagation.

Early ray tracing programs were primarily concerned with integrating the ray tracing equations of the next section accurately and efficiently. It is shown that the effect of sound-speed representations on the computed value of propagation loss is not as important as is currently believed. The most recent addition to practical ray tracing programs is the asymptotic treatment of caustics.

In the case of a horizontally stratified ocean, the integral representation may be expanded into a multipath series, each term of which corresponds to a particular ray type. Upon integrating, one obtains the acoustic pressure along the ray. It is important to note that this multipath expansion is exact. The accuracy of the final result depends on the method of solving the depth dependent wave equation and evaluating the ray type integrals.

For low frequency propagation in nearly horizontally stratified oceans, the method of horizontal rays is recommended. Here, the pressure is expressed as a summation of normal modes weighted by amplitudes satisfying horizontal ray tracing equations.

### RAY TRACING EQUATIONS

Several years ago, the state of the art was described in Officer's<sup>1</sup> book on sound transmission. Then, ray tracing involved approximating the solution of the reduced wave equation for the acoustic pressure  $P$

$$\nabla^2 P + \left(\frac{\omega}{c}\right)^2 P = 0$$

with the Wentzel-Kramers-Brillouin-Jeffreys (WKBJ) form

$$P = a \exp(i\omega T) .$$

The travel time  $T$  and amplitude  $a$  satisfy the eikonal equation

$$(\nabla T)^2 = c^{-2}$$

and the transport equation

$$\nabla \cdot a^2 \nabla T = 0 ,$$

respectively.

The eikonal equation may be solved by using the method of characteristics for first-order partial differential equations. Characteristic curves, better known as rays, are orthogonal to surfaces of constant time. They satisfy the ray tracing equations

$$\frac{d}{ds} \left( \frac{1}{c} \frac{dx}{ds} \right) = \frac{\partial}{\partial x} \frac{1}{c}$$

$$\frac{d}{ds} \left( \frac{1}{c} \frac{dy}{ds} \right) = \frac{\partial}{\partial y} \frac{1}{c}$$

$$\frac{d}{ds} \left( \frac{1}{c} \frac{dz}{ds} \right) = \frac{\partial}{\partial z} \frac{1}{c}$$

$$\frac{dT}{ds} = \frac{1}{c}$$

$$\left( \frac{dx}{ds} \right)^2 + \left( \frac{dy}{ds} \right)^2 + \left( \frac{dz}{ds} \right)^2 = 1 .$$

Once the rays have been found, the divergence theorem applied to the transport equation produces the geometrical spreading law for the pressure amplitude,

$$\frac{a}{a_0} = \left( \frac{c_0}{c} \frac{\delta \sigma}{\delta \sigma_0} \right)^{-1/2} ,$$

or for the equivalent plane wave intensity,



$$\frac{I}{I_0} = \left( \frac{\delta \sigma}{\delta \sigma_0} \right)^{-1} .$$

The subscript zero refers to a reference point (usually 1 yd away from a point source), and  $\delta \sigma$  is the cross-sectional area of an infinitesimal ray tube. The intensity satisfies the conservation of energy law along a ray tube. It can be shown that pressure, on the other hand, satisfies the law of reciprocity.

In the case of a horizontally stratified ocean, that is, the sound speed and ocean boundaries are independent of both horizontal coordinates, the rays remain in a vertical plane and obey Snell's law,

$$\frac{1}{c} \frac{dr}{ds} = \text{constant} ,$$

where

$$r^2 = x^2 + y^2 .$$

### SOUND SPEED REPRESENTATIONS

When ray theory was first implemented on digital computers, the primary concern was to integrate the ray tracing equations accurately and efficiently. Pedersen<sup>2</sup> motivated the design of many ray tracing programs by demonstrating the fact that discontinuities in the sound speed gradient could introduce anomalies in the computed value of geometrical spreading loss.

This effect is illustrated by fitting the sound speed profiles of figure 1 with piecewise linear,<sup>1</sup> piecewise quadratic,<sup>2</sup> and cubic spline<sup>3</sup> representations. Differences are more readily seen in the sound speed gradients shown in this figure. The corresponding ray diagrams, figure 2, show that caustics due to discontinuities in the gradient of the piecewise linear fit disappear when smoother sound speed representations are employed. Propagation losses computed according to classical ray theory tend to accentuate this effect, but consider what would happen if a ray theory generalized to treat caustics correctly were used instead. Figure 3 indicates that the effect of different sound speed representations is insignificant providing that each representation accurately describes the input data to be fitted.

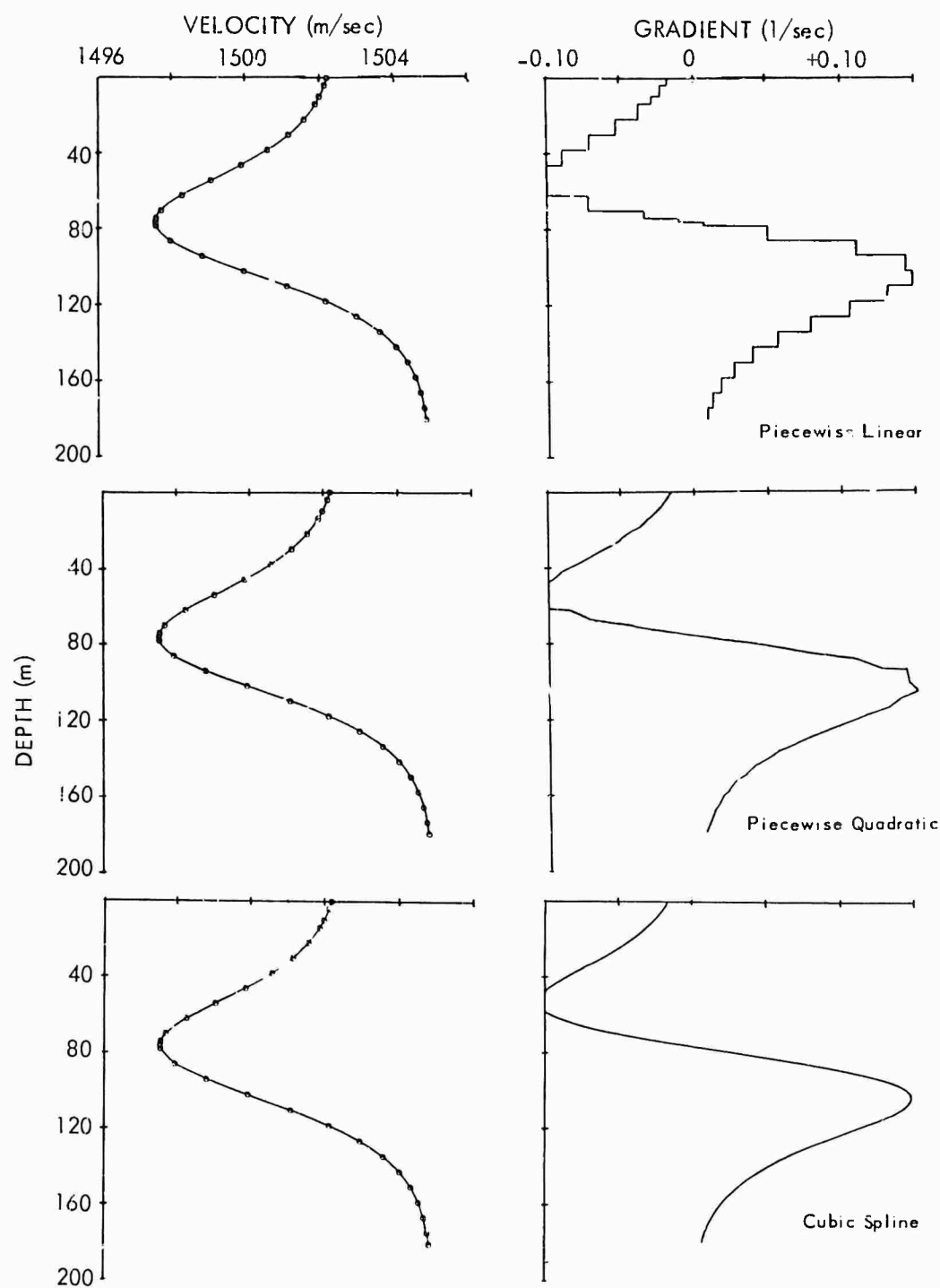


Figure 1. Comparison of Sound Speed Representations and Gradients

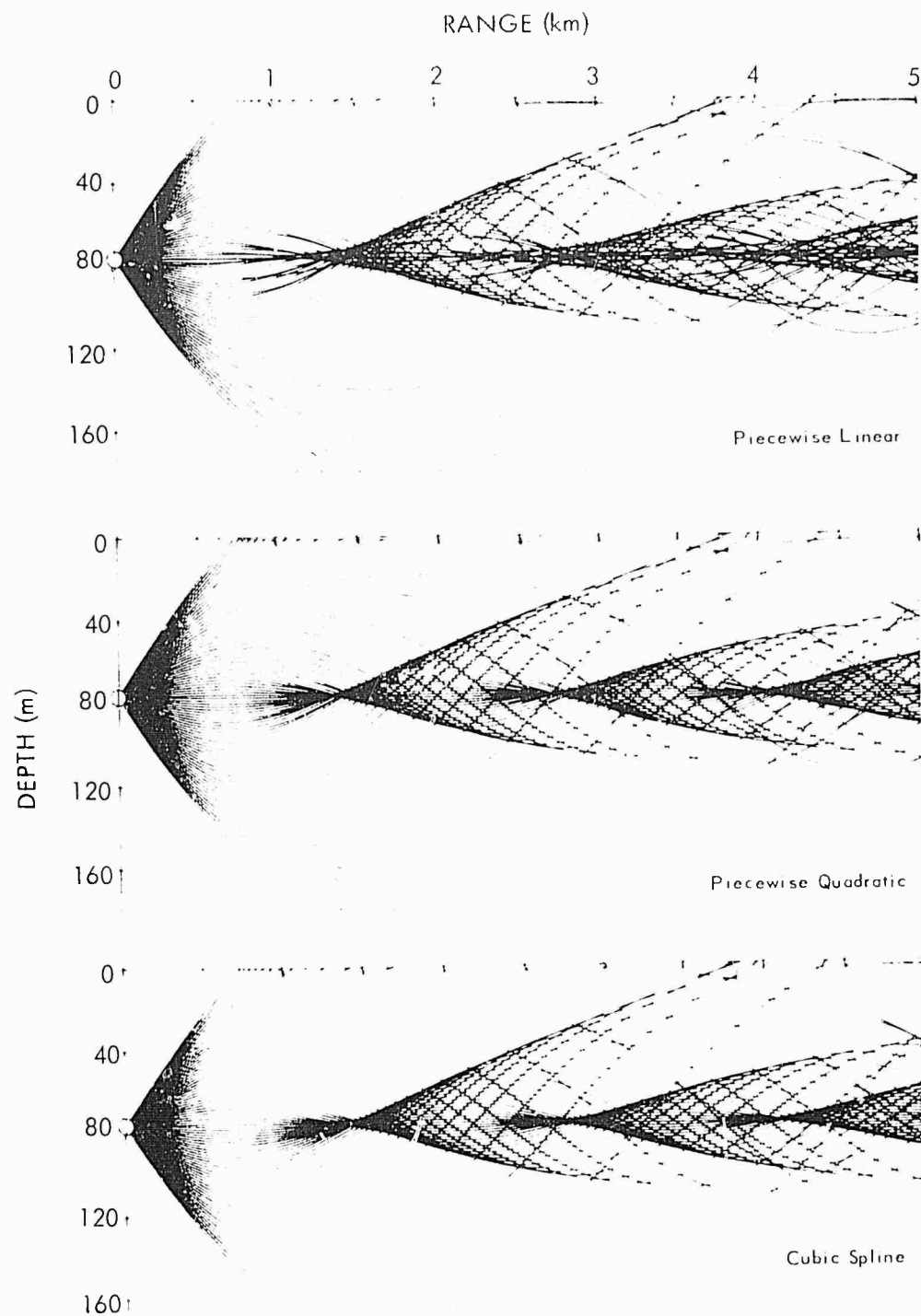


Figure 2. Comparison of Ray Diagrams for an Axial Source

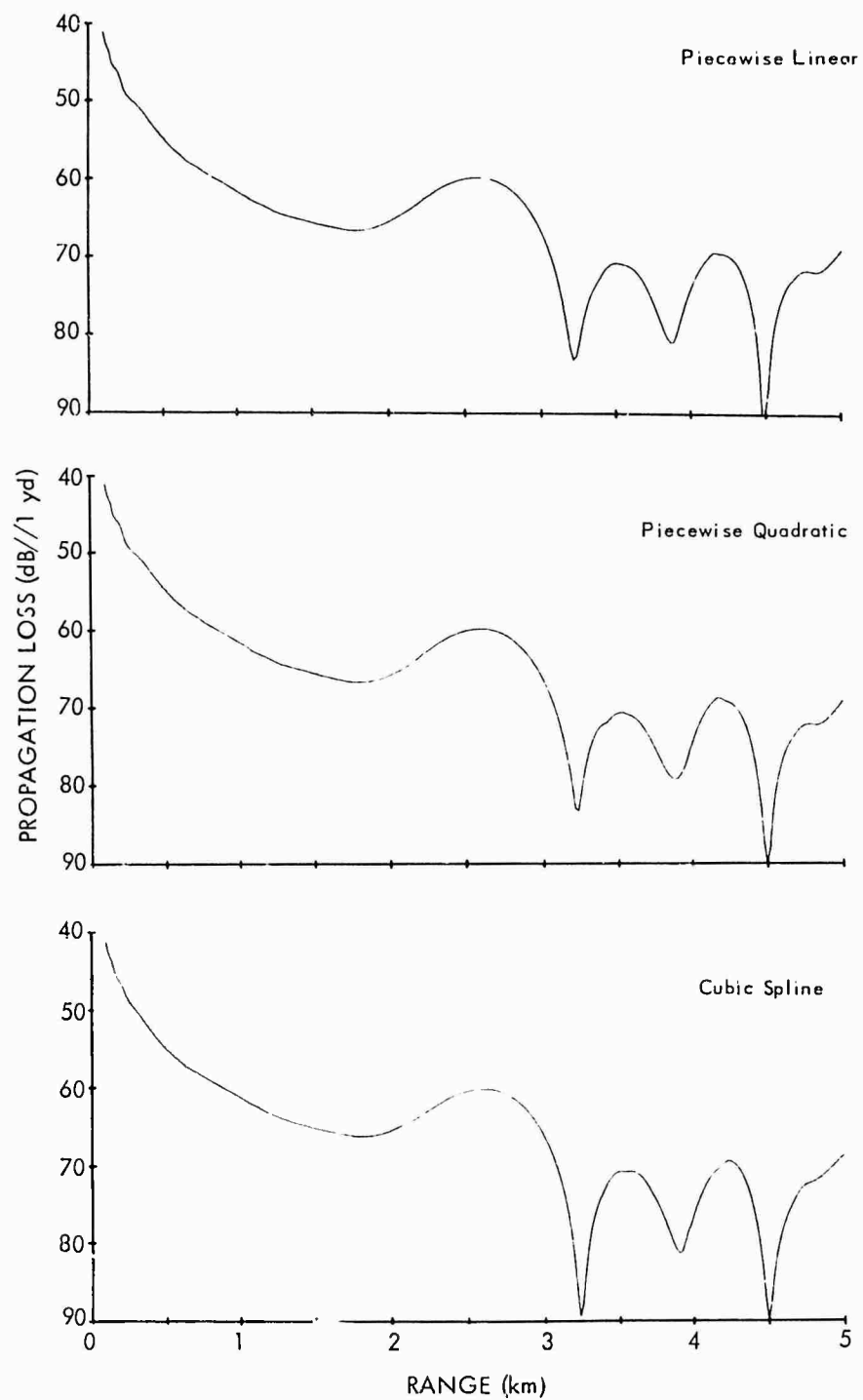


Figure 3. Comparison of 1-kHz Propagation Losses for a 40-m Receiver Depth

As far as ray diagrams and propagation losses computed according to classical ray theory are concerned, past experience indicates that cubic splines produce the best representations for analytic type sound speeds. However, as the input data become more irregular, the curve fitting procedure becomes more difficult to automate.<sup>4</sup> A second disadvantage of cubic splines is that the corresponding ray tracing equations cannot be integrated in closed form, which is a process that can be accomplished with piecewise linear and quadratic fits.

Many of the statements made above are also true when the sound speed varies with one or more horizontal coordinates as well as depth. If, for example, the input data are fitted with triangular planes, the ray tracing equations may be integrated in closed form, but anomalies due to discontinuous gradients are possible.

#### ASYMPTOTIC TREATMENT OF CAUSTICS

In the last few years, significant advances in practical ray tracing techniques involved the treatment of caustics rather than improvements in curve fitting algorithms. The problem may be illustrated when the sound speed decreases inversely as the square root of depth, as shown in figure 4. We see that the ray diagram, figure 5, forms a well defined caustic.

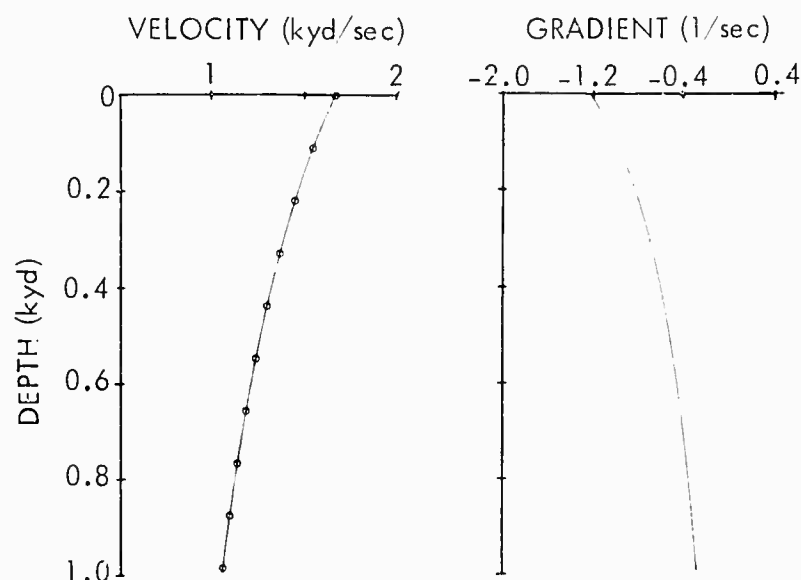


Figure 4. Sound Speed and Gradient Studied by Pedersen and Gordon

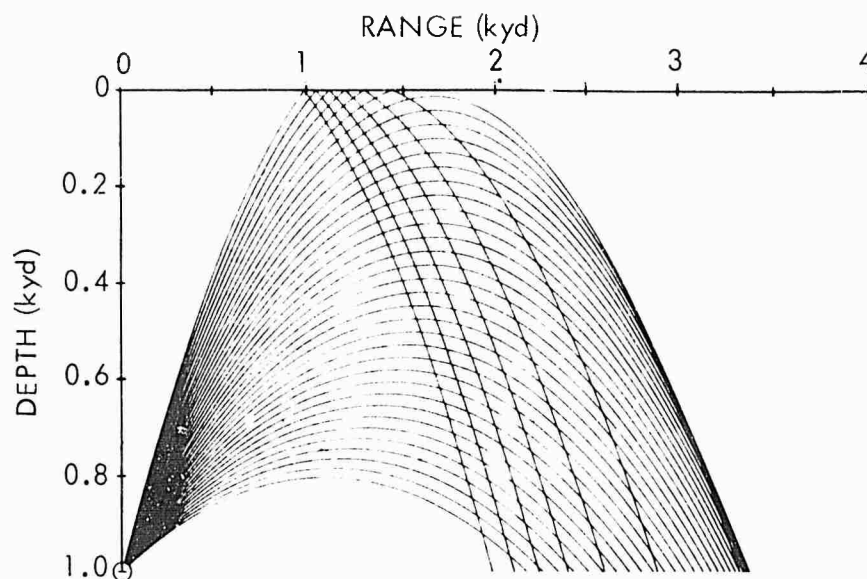


Figure 5. Ray Diagram for a 1-kyd Source Depth  
Computed by Using the Sound Speed of Figure 4

Pedersen and Gordon<sup>5</sup> compared the classical solution (solid line) with Brekhovskikh's<sup>6</sup> modified ray theory (broken line) in figure 6. Classical ray theory predicts an infinite intensity at the caustic at 3159 yd and an infinite propagation loss in the shadow zone to the right of the caustic. Pedersen and Gordon explain that the abrupt change in loss at 3130 yd occurs at the ray that grazes the ocean surface. The modified ray theory did not apply to the left of this ray.

The above remark points out the difficulty of applying modified ray theories to the simplest of caustic geometries. Additional effects due to the ocean boundaries, cusped caustics, etc., prevent the theory from being applicable everywhere. One can program as many special cases as practical considerations suggest, but, more often, one uses classical and modified theories outside their domain of validity. Since caustic corrections are usually obtained by including additional terms of a high frequency expansion, errors increase as the frequency decreases.

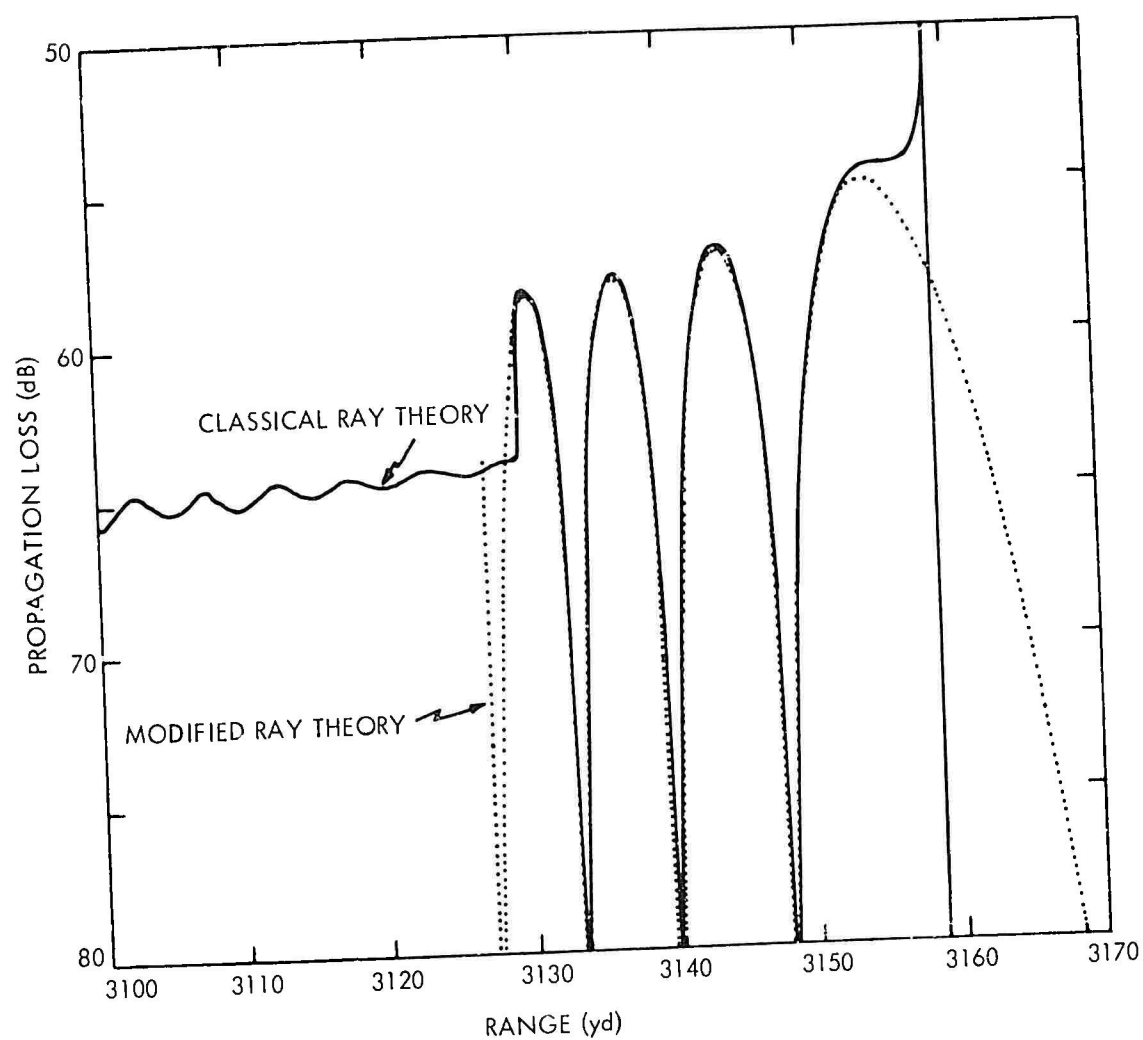


Figure 6. Comparison of 2-kHz Propagation Losses for a 0.8-kyd Receiver Depth Computed According to Classical and Modified Ray Theories (After Pedersen and Gordon, reference 5.)

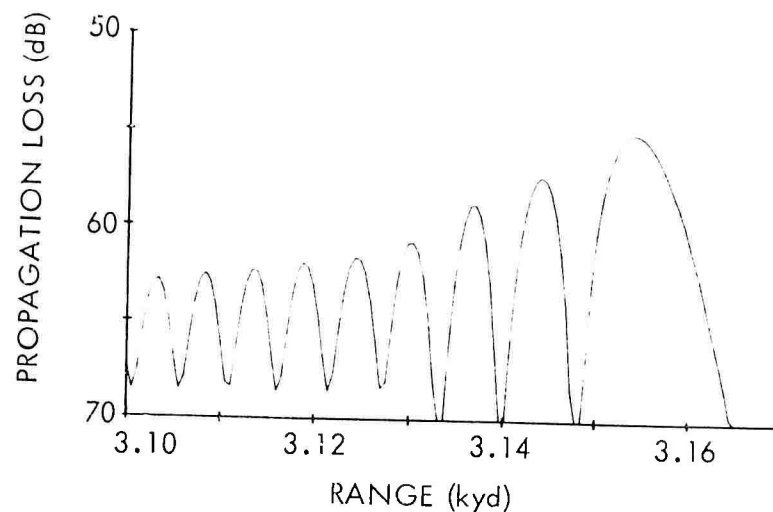


Figure 7. Propagation Loss for a 0.8-kyd Receiver Depth  
Computed More Accurately Than That for Classical or  
Modified Ray Theories

Consider what would happen if a theory generalized to treat caustics correctly were used instead. The result, figure 7, indicates that there is no discontinuity in propagation loss at the ray that grazes the ocean surface and also that classical ray theory appears to be more accurate to the right of the grazing ray than to the left. Consequently, modified ray techniques should be exercised with caution.

Spofford was one of the first to implement modified ray theory in a practical computer program. The procedure, based on the work of Ludwig,<sup>7</sup> assumes that the reduced wave equation has an asymptotic solution of the form

$$P = \exp(i\omega T) \left\{ g A_i(\omega^{2/3} \rho) + \frac{h}{i\omega^{1/3}} A_i'(\omega^{2/3} \rho) \right\}$$

subject to the orthogonality condition

$$\nabla T \cdot \nabla \rho = 0 ,$$



where  $Ai$  is the Airy function of the first kind, and  $T$ ,  $\rho$ ,  $g$ , and  $h$  are to be found. Upon substituting this ansatz into the reduced wave equation and comparing similar powers of frequency, one obtains

$$\begin{aligned} T &= (T_+ + T_-)/2, \\ 2/3 \rho^{3/2} &= (T_+ - T_-)/2, \\ g &= \rho^{1/4} (a_+ + a_-)/2, \\ h &= \rho^{-1/4} (a_+ + a_-)/2. \end{aligned}$$

As illustrated in figure 8, subscripts  $+$  and  $-$  refer to the two rays that touch and do not touch the caustic before reaching the field point, respectively. Therefore, all the quantities appearing in Ludwig's representation may be expressed in terms of the travel times  $T_{\pm}$  and amplitudes  $a_{\pm}$  of classical ray theory. Brekhovskikh's solution lacks the term involving the Airy function derivative, a term that is important away from the caustic. As a result, Ludwig's solution has a larger domain of validity.

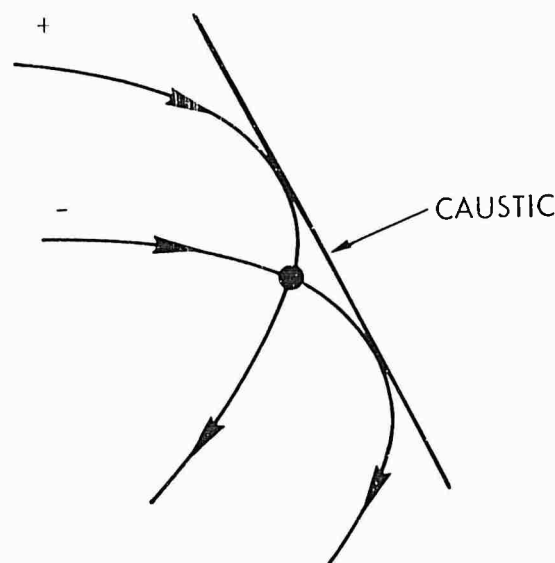


Figure 8. Classical Rays Used to Compute a Uniform Asymptotic Solution at a Caustic

# LOW FREQUENCY PROPAGATION IN HORIZONTALLY STRATIFIED OCEANS

Most of the figures discussed before were produced by a computer program designed to model acoustic propagation in a horizontally stratified ocean. For mediums such as this, the acoustic pressure due to a unit point harmonic source situated at  $(0, 0, z_S)$  has the integral representation

$$P(r, z, z_S; \omega) = \omega \int_0^\infty \omega \lambda J_0(\omega \lambda r) G(z, z_S; \lambda, \omega) d\lambda,$$

where the Green's function  $G$  satisfies the depth dependent wave equation

$$\left[ \partial^2 / \partial z^2 + \omega^2 \left\{ c^{-2}(z) - \lambda^2 \right\} \right] G(z, z_S; \lambda, \omega) = -2\delta(z - z_S)$$

and suitable boundary conditions.

The method of solution used here, that is multipath expansion of the integral representation, is quite old, dating back nearly 40 years to Van der Pol and Bremmer.<sup>8</sup> Following Leibiger and Lee,<sup>9</sup> the Green's function is expressed in terms of two linearly independent solutions  $F_+$  of the homogeneous depth dependent equation. The solutions  $F_-$  are normalized so that their Wronskian equals  $-2\omega i$ . Upon expanding the denominator of  $G$  into a geometric series, the double summation

$$P(r, z, z_S; \omega) = \sum_{\nu=0}^{\infty} \sum_{n=1}^4 P_n^{(\nu)}(r, z, z_S; \omega)$$

is obtained. If  $z < z_S$ , one sees that

$$P_n^{(\nu)}(r, z, z_S; \omega) = \int_0^\infty i\omega J_0(\omega \lambda r) F_-(z; \lambda, \omega) F_+(z_S; \lambda, \omega) \gamma_{\text{sur}}^\nu(\lambda, \omega) \gamma_{\text{bot}}^\nu(\lambda, \omega) d\lambda,$$

where  $\gamma_{\text{sur}}$  and  $\gamma_{\text{bot}}$  are boundary reflection coefficients. Other terms of the series are similar, each integral representing a particular ray type. The first four are illustrated in figure 9. It is important to note that, so far, the solution is exact. The validity of the final result depends on the method of

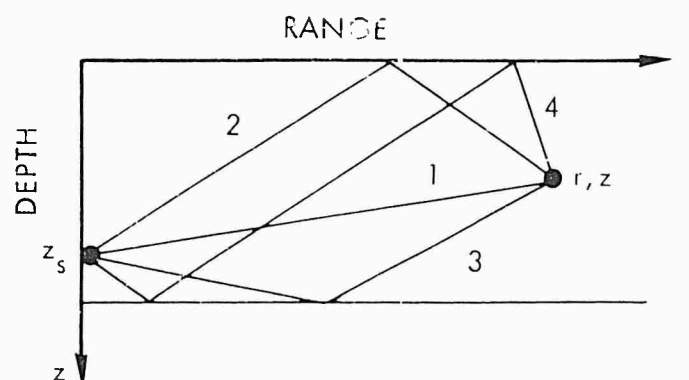


Figure 9. The Principal Ray Types

solving the depth dependent wave equation and evaluating the ray type integrals. If WKBJ and stationary phase techniques are used, respectively, the classical ray theoretic solution is obtained. Murphy<sup>10</sup> replaced the WKBJ technique with a Weber function representation in order to treat the two-turning-point problem. Brekhovskikh replaced the method of stationary phase with an Airy integral modification in order to investigate caustics.

At present, our propagation model uses the following modified WKBJ expression to solve the depth dependent wave equation:

$$F_{\pm}(z; \lambda, \omega) = \pi^{1/2} \omega^{1/6} \exp \left\{ \pm i \omega Q(z_0, z_t; \lambda) \mp i \pi/4 \right\} \\ g(z; \lambda) \left( \text{Bi} \left\{ \omega^{2/3} \rho(z; \lambda) \right\} \pm i \text{Ai} \left\{ \omega^{2/3} \rho(z; \lambda) \right\} \right),$$

$$Q(z_0, z_t; \lambda) = \int_{z_0}^{z_t} \left\{ c^{-2}(\xi) - \lambda^2 \right\}^{1/2} d\xi,$$

$$\rho(z; \lambda) = - \left\{ \frac{3}{2} Q(z, z_t; \lambda) \right\}^{2/3}, \text{ and } g(z; \lambda) = \left| \frac{\partial \rho(z; \lambda)}{\partial z} \right|^{-1/2},$$

where

$z_0$  is a suitably chosen reference point

$z_t$  is a turning point

$Bi$  is the Airy function of the second kind.

Whenever  $\omega^{2/3} p$  is a moderate to large negative number,  $F_{\pm}$  reduces to the usual WKB representation

$$F_{\pm}(z; \lambda, \omega) = \left\{ e^{-2} (z) - \lambda^2 \right\}^{-1/4} \exp \left\{ \pm i \omega Q(z_0, z; \lambda) \right\}.$$

Since this modified representation is inaccurate in the vicinity of double turning points,  $F_{\pm}$  are arbitrarily set to zero whenever they occur. Hopefully, this will only affect a small interval of integration and will not introduce significant errors in the final result. Murphy's technique offers an alternative procedure.

The method of evaluating the ray type integrals is based on the following:

1. Segment the interval of integration into suitably chosen subintervals.
2. Use stationary phase to evaluate subintegrals whenever possible.
3. Integrate the remaining cases numerically.

It was originally thought that the numerical integration, although lengthy when compared with stationary phase, would be invoked so infrequently that its contribution to the total computer running time would be inconsequential. So far, this has not been the case. Hopefully, the running time will be reduced eventually when the integration routine is made more efficient.

Since it is customary to give computer programs names so that they may be distinguished from others performing similar functions, the program used herein is called CONGRATS V, where CONGRATS is an acronym for Continuous Gradient Ray Tracing System. Actually, the completed program will predict the performance of active and passive sonar systems and is, therefore, more than just a propagation program. As shown in figures 1 through 3, CONGRATS V has the option to invoke several ray tracing procedures. The propagation losses were obtained by adding the multipath contributions coherently. CONGRATS V also produces a plot of propagation loss using power addition, in which case the phases of the individual contributors are neglected.

## A COMPARISON OF PROPAGATION MODELS

At present, the state of the art of propagation modeling for stratified oceans may be illustrated by two figures compiled by E. Jensen of NUSC. (See figures 10a and 11a.) Both compare FFP,<sup>11</sup> FACT,<sup>12</sup> RAYMODE 9,<sup>13</sup> and NISSM II<sup>14</sup> computer predictions for 50-Hz propagation in the Pacific. The choice of programs included in the comparison was mainly of convenience, since each is available at NUSC, New London, and all but FACT were designed there.

Briefly, the Fast Field Program (FFP) utilizes Fast Fourier Transforms to evaluate the integral representation. The Fast Asymptotic Coherent Transmission Model (FACT) is a constant gradient ray tracing program incorporating sophisticated low frequency modifications. RAYMODE 9, the latest version of the series, uses ray theory to determine which intervals dominate the integral representation, but uses normal modes to compute the acoustic amplitude. The Navy Interim Surface Ship Model (NISSM) II is a continuous gradient ray tracing program designed to predict the performance of active sonar systems. All but FFP have the option to combine multipath contributions incoherently as well as coherently, and all but FFP use alternative procedures for surface duct propagation.

As a result, the first case (figure 10a), which is dominated by surface duct propagation, will show the greater variability. FACT is an order of magnitude faster than NISSM II and RAYMODE 9, while FFP is a good deal slower.

Upon adding CONGRATS V to the comparison (figure 10b) and invoking the coherent phase option, one sees good agreement with FFP. Had the incoherent phase option been invoked instead, CONGRATS V would have agreed with the others.

The second case, figure 11a is dominated by convergence zone propagation. The agreement is better than before although running times continue to differ by orders of magnitude.

Upon adding CONGRATS V to this comparison (figure 11b), one obtains reasonable agreement with FFP. It is unusual to find agreement among models that are based upon different theories and written by different programmers. Unfortunately, comparisons are not always this good. Hopefully, all discrepancies will soon be eliminated or at least accounted for.

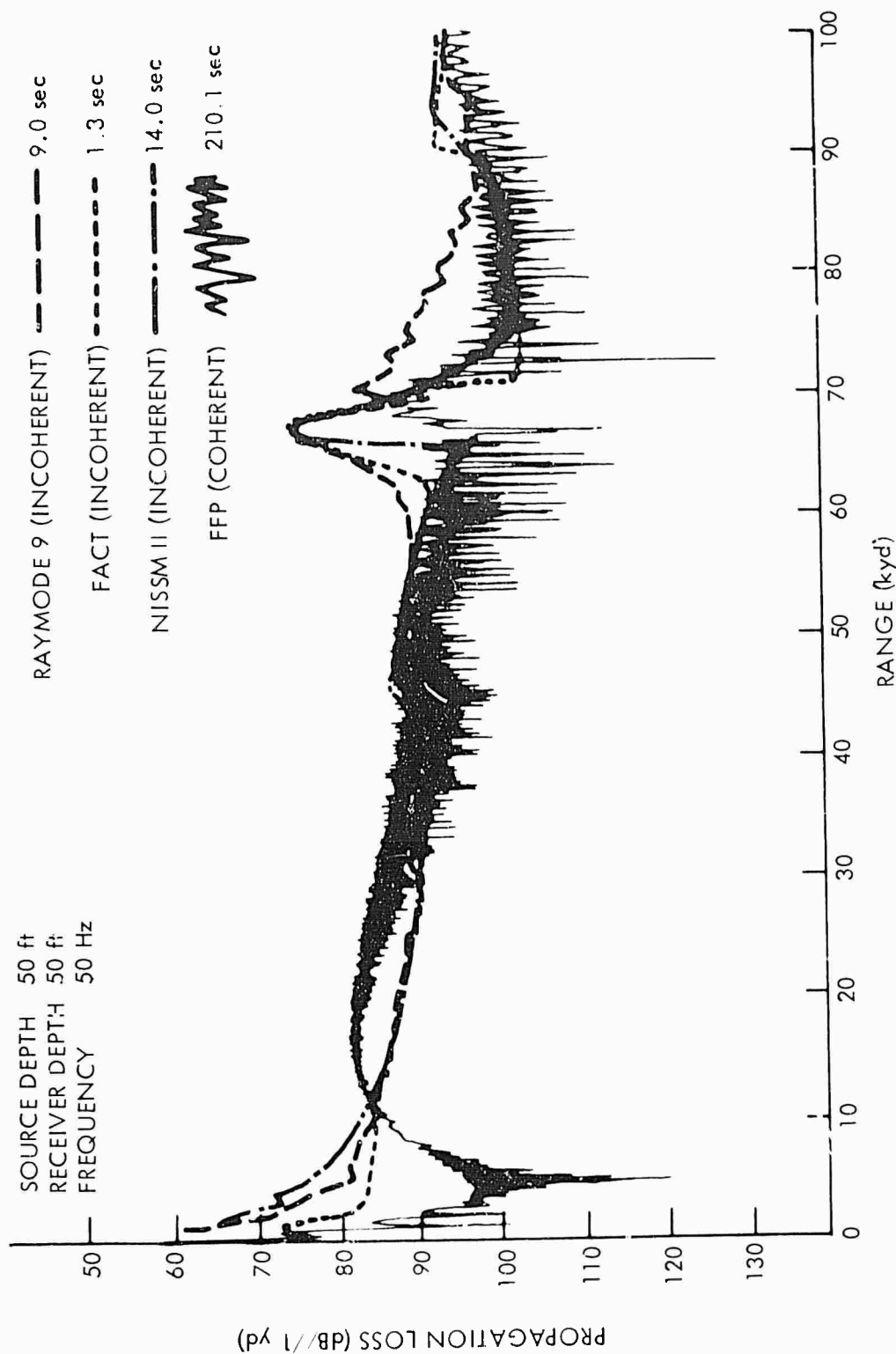


Figure 10a. Low Frequency Surface Duct Propagation for a Pacific Sound Speed Profile  
 (From E. Jensen, of NUSC, unpublished data.)

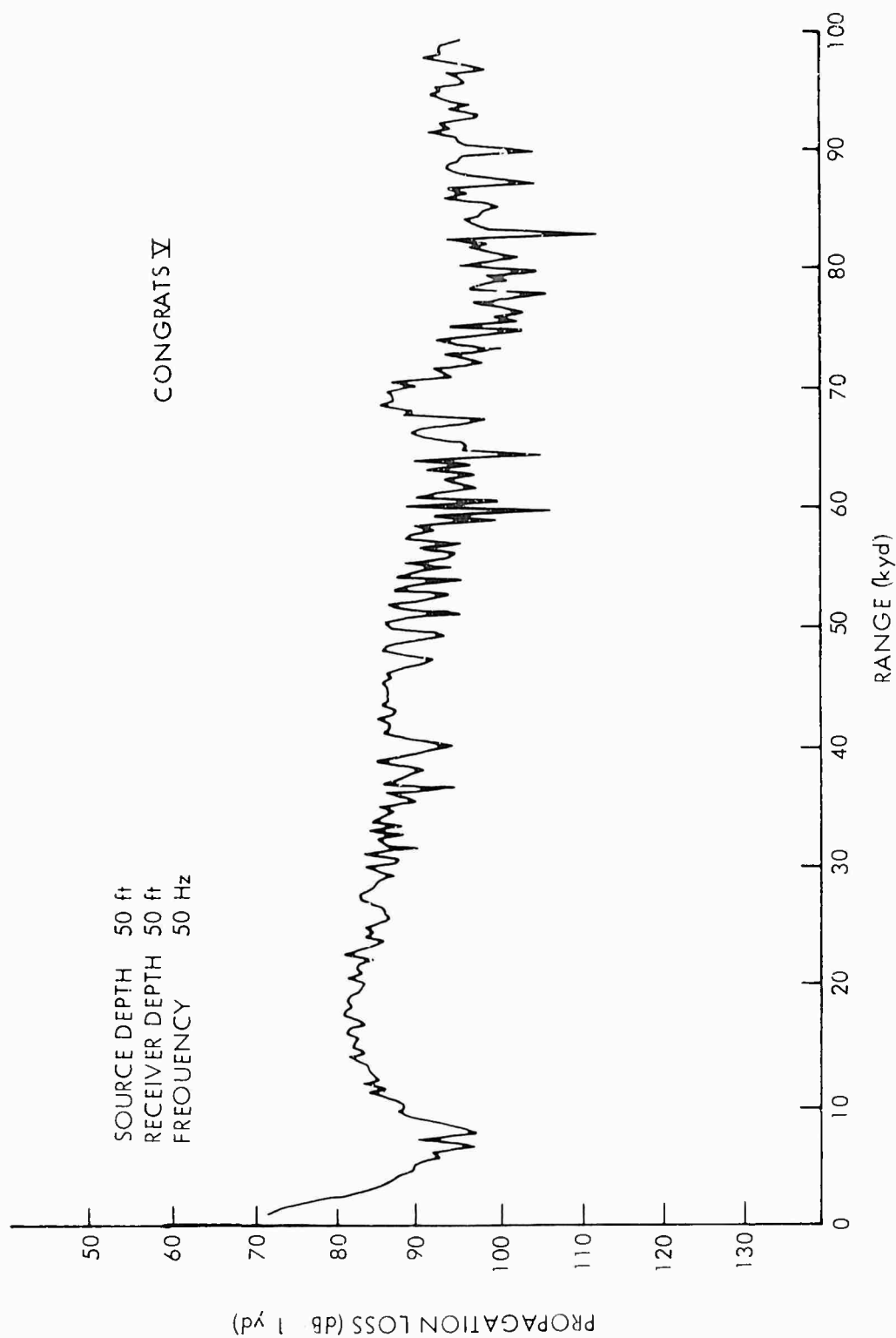


Figure 10b. CONGRATS V Low Frequency Surface Duct Propagation for a Pacific Sound Speed Profile

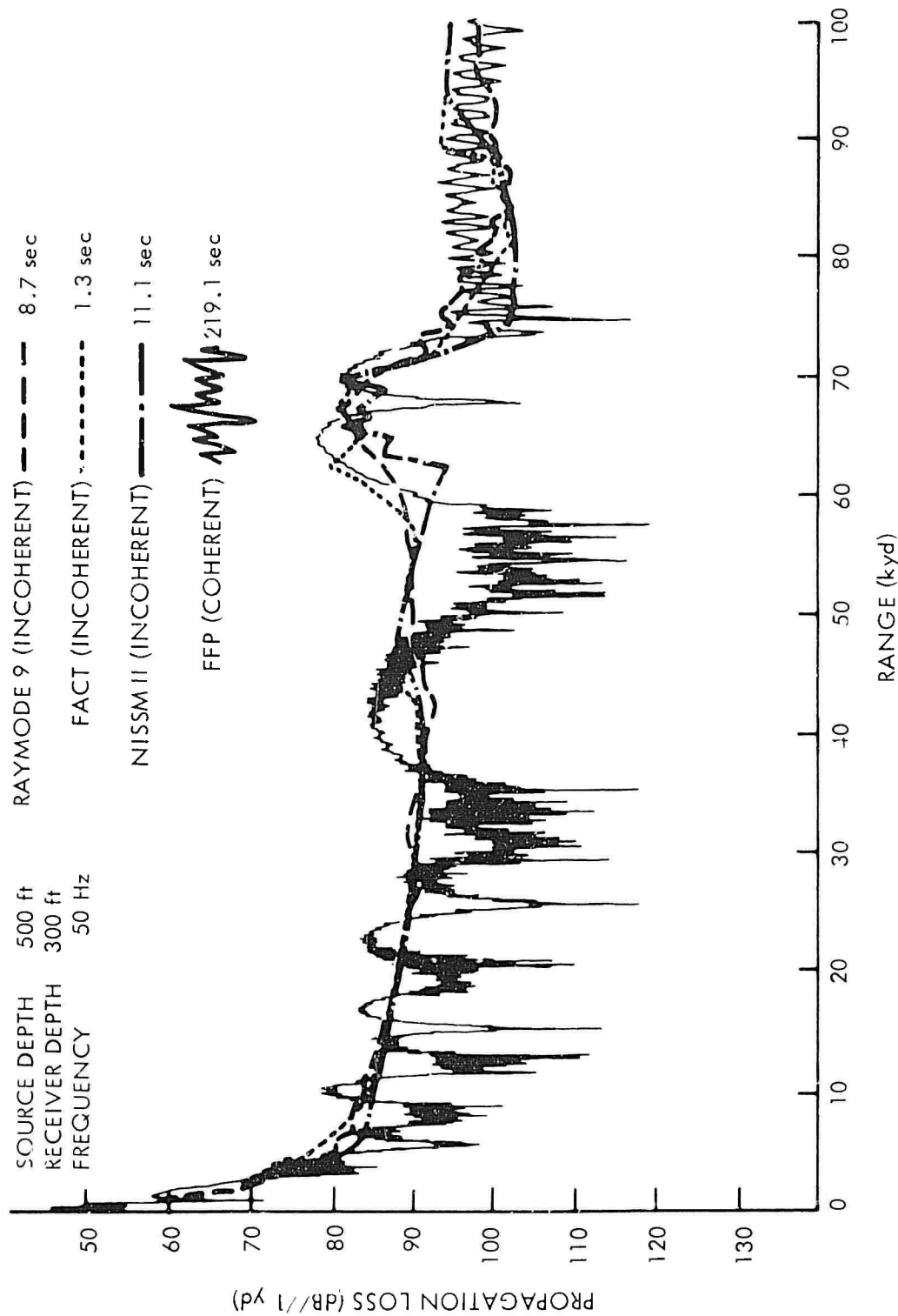


Figure 11a. Low Frequency Convergence Zone Propagation for a Pacific Sound Speed Profile  
 (From E. Jensen, of NUSC, unpublished data.)



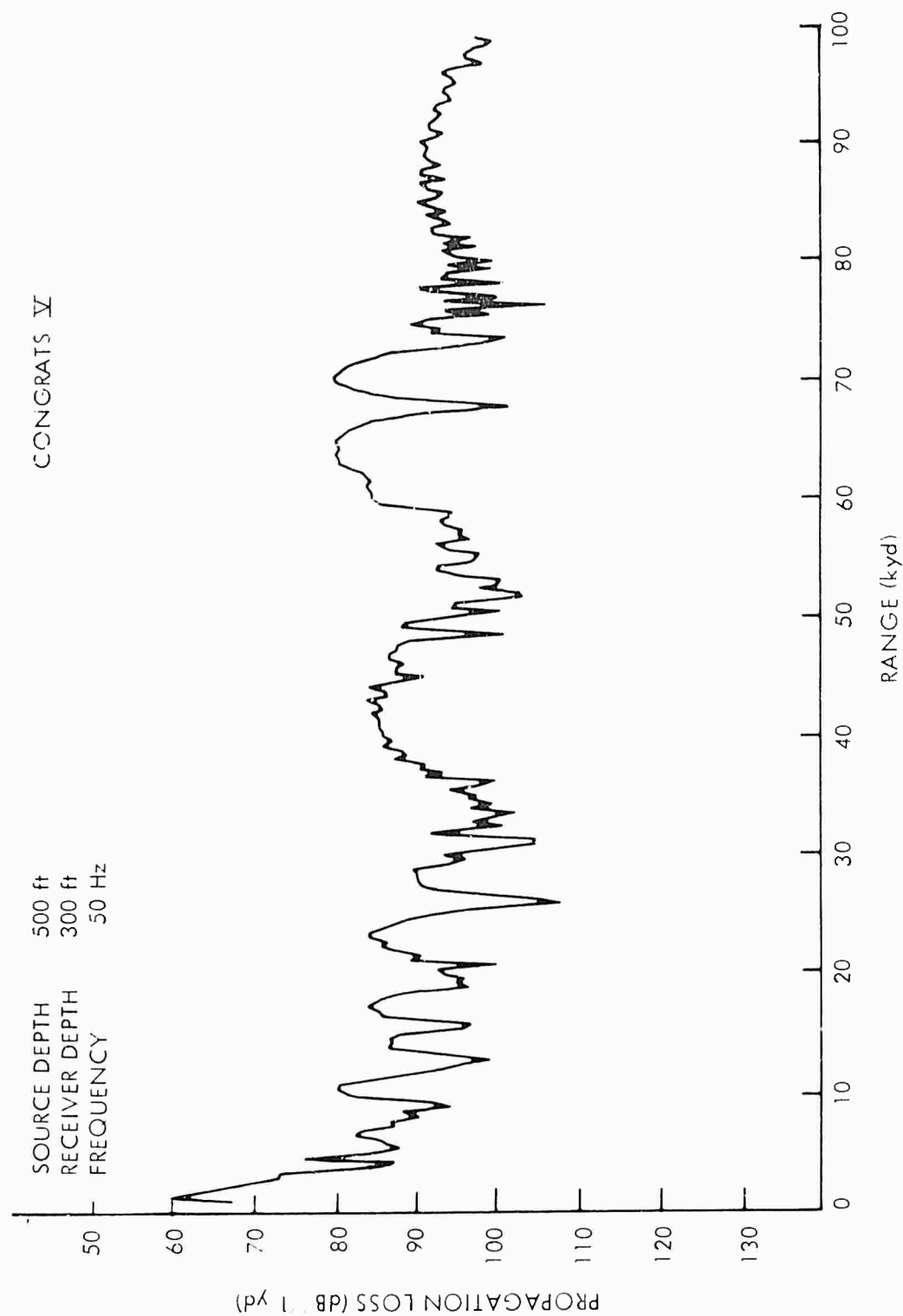


Figure 11b. CONGRATS V Low Frequency Convergence Zone Propagation for a Pacific Sound Speed Profile

# HORIZONTAL RAY THEORY FOR NEARLY HORIZONTALLY STRATIFIED OCEANS

At long ranges or in shallow water, the effects of horizontal variations in the sound-speed or bottom characteristics are often large and not readily modeled by any of the techniques discussed previously. A nearly horizontally stratified ocean is one in which the horizontal variation is slow.

This rather vague notion is quantized by introducing a small parameter  $\epsilon$  and assuming that the properties of the medium depend on the horizontal coordinates  $X, Y$  only through the combinations<sup>15</sup>

$$x = \epsilon X, \quad y = \epsilon Y.$$

This being so, let us seek solutions of the reduced wave equation in the form

$$P(x, y, z; \epsilon) \approx \exp \{ \theta(x, y)/i\epsilon \} \sum_{\nu=0}^{\infty} A_{\nu}(x, y, z) (i\epsilon)^{\nu}.$$

Each  $A_{\nu}$ , in turn, is assumed to have the form

$$A_{\nu}(x, y, z) = \sum_{k=0}^{\infty} a_{\nu}^{(k)}(x, y) \psi_k(x, y, z),$$

where the  $\psi_k$  are orthonormal eigenfunctions of the depth dependent wave equation

$$\frac{\partial^2 \psi_k}{\partial z^2} + K^2(x, y, z) \psi_k = \lambda_k^2 \psi_k$$

subject to the appropriate boundary conditions.

Upon substituting our ansatz into the reduced wave equation and comparing similar powers of  $i\epsilon$ , one finds that the phase function,  $\theta$ , satisfies the horizontally dependent eikonal equation

$$\left( \frac{\partial \theta}{\partial x} \right)^2 + \left( \frac{\partial \theta}{\partial y} \right)^2 = \lambda_p^2(x, y),$$

where  $\lambda_p$  is one of the eigenvalues,  $\lambda_k$ , computed above.

This equation, like the ordinary eikonal equation, may be solved by using ray tracing techniques. Note, however, that all depth dependence is missing. The pressure depends on depth only through the vertical eigenfunctions. It may also be shown that the leading amplitude,  $a_p^{(0)}$ , satisfies the conservation law

$$\lambda_p \left( \frac{a^{(0)}}{p} \right)^2 \delta \sigma = \text{constant}$$

along a horizontal ray tube.

A computer program based on the consideration above was written to proceed in two stages. The first determines the eigenvalues and normalized eigenfunctions at each point of a rectangular grid in the horizontal plane. Then, during the second part, a set of horizontal ray tracing equations is integrated for each eigenvalue, and the contributions of individual modes are combined to obtain the total field.

As in ordinary ray programs, only the leading term of the asymptotic expansion of each mode is found. The expansion then reduces to that derived by Pierce almost 10 years ago.<sup>16</sup>

The program predicted propagation loss along a 1500-nmi track extending northward from 27° 30'N, 157° 50'W to 52° 30'N, 157° 59'W. Eleven equidistant velocity-depth profiles obtained from the measured data displayed in figure 12 were entered into the computer program. Note that the SOFAR axis rises from a depth of 795 m at 27° 30'N to about 50 m at 52° 30'N. Lack of relevant data prevented the inclusion of any dependence of sound speed or bottom depth upon longitude.

Figure 13 displays propagation losses from dynamite charges detonated 500 ft below sea level along the track to a 2500-ft receiver depth situated at 27° 30'N. The top graph represents observational data, while the middle graph shows computed results. The two are superimposed in the bottom graph. The figure displays an interesting feature. The propagation loss decreases with increasing range beyond 42°N. This decrease may be explained by the fact that the receiver is only 124 ft away from the SOFAR axis, where the signal is strongly affected by the amplitude of the few lowest modes, as shown in figure 14. As the source ship moved north, the source approached the SOFAR axis causing the amplitude of these modes (figure 15) to increase to such an extent that eventually the loss due to horizontal spreading was overcome and the total propagation loss decreased.

The 70,800-ft receiver depth of figure 16 is well below the turning points of the first few modes, and so the signal there is dominated by the higher modes. The amplitudes of these modes are not greatly affected when the source approaches the SOFAR axis; therefore, for this receiver, cylindrical spreading dominates the entire track.

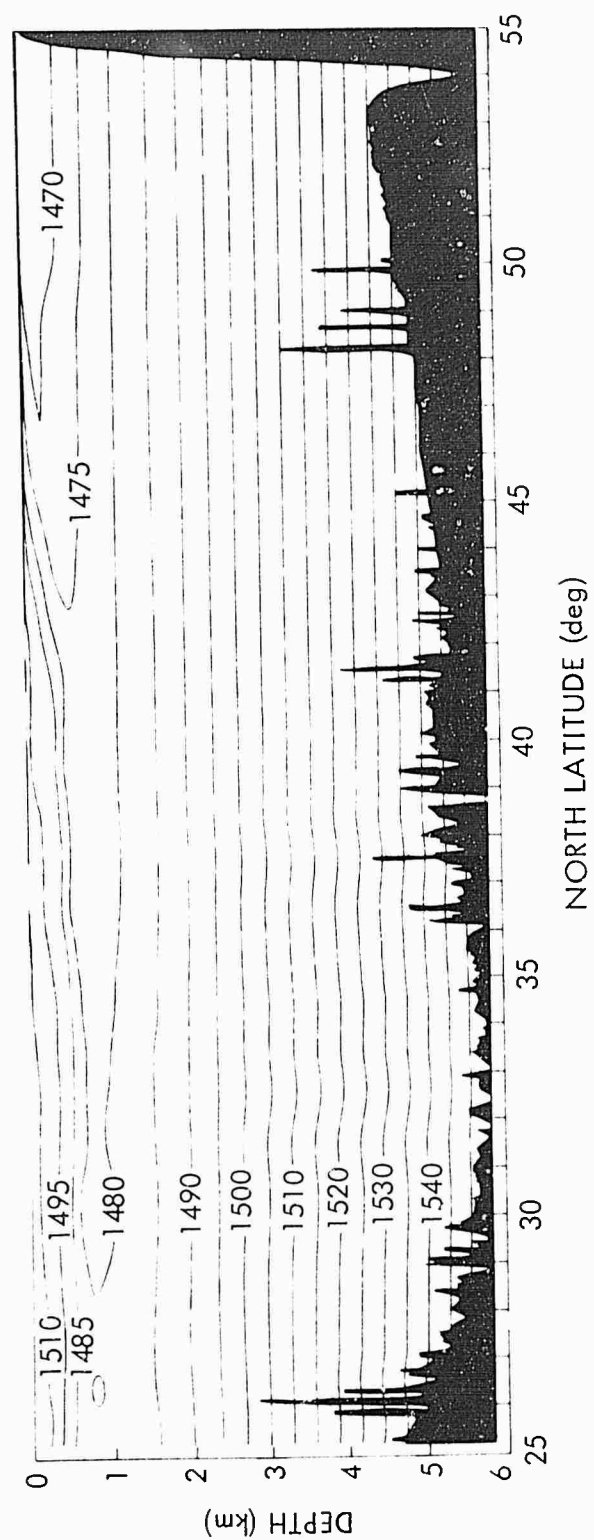


Figure 12. Contour of Sound Speed (m/sec) Along the Meridian 157° 50'W

FREQUENCY 31 Hz  
SOURCE 500 ft  
RECEIVER 2500 ft

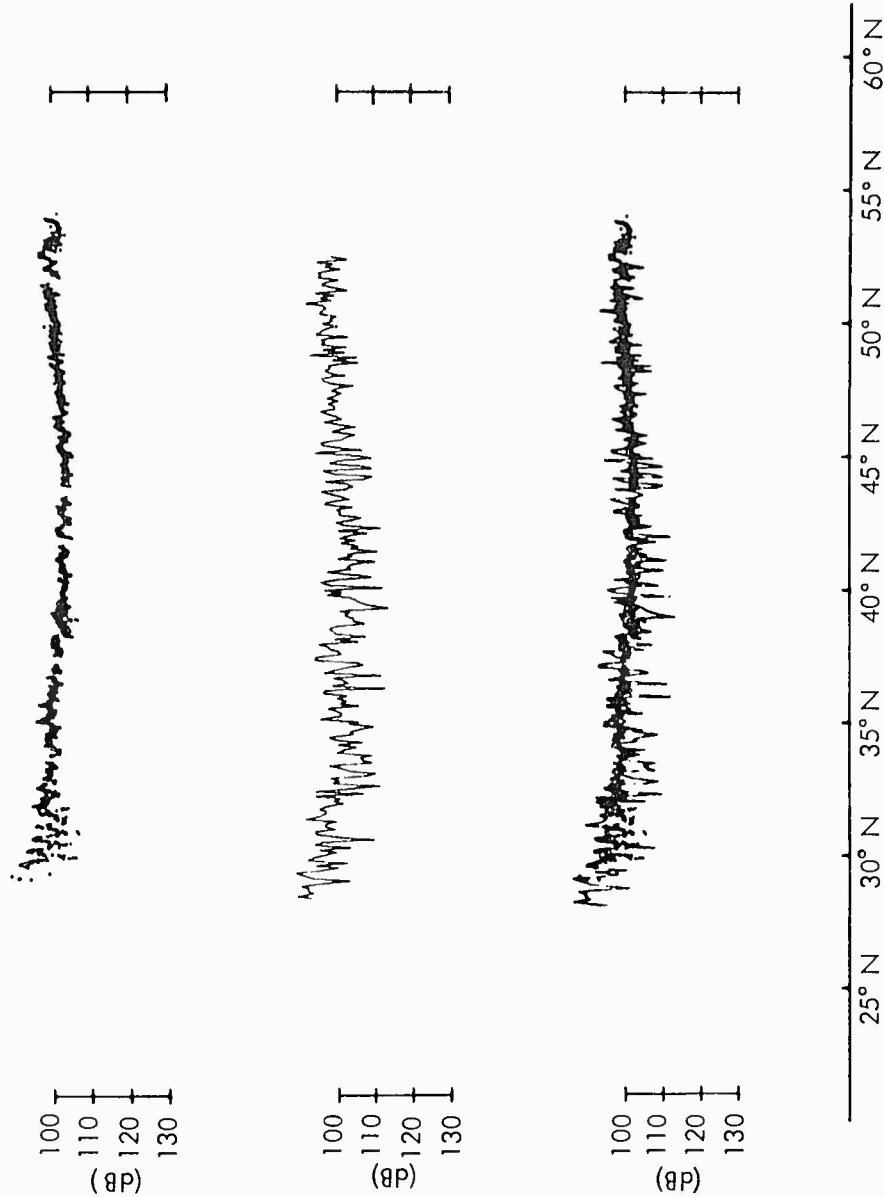


Figure 13. Propagation Loss versus Range for a 2500-ft Receiver Depth, a 500-ft Source Depth, and a 31-Hz Frequency

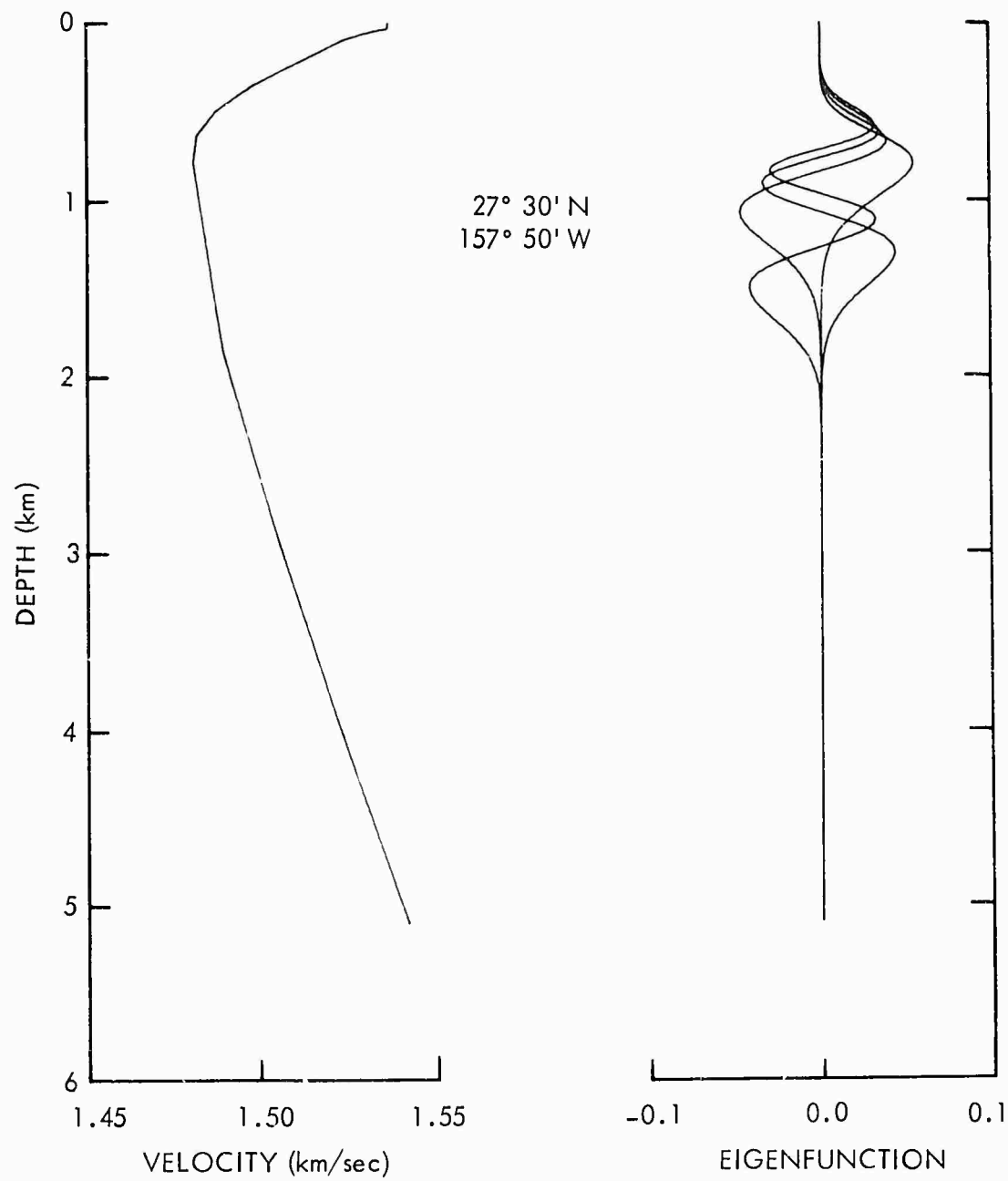


Figure 14. Sound Speed-Depth Profile at  $27^{\circ} 30' N$ ,  $157^{\circ} 50' W$  and the Corresponding First Four Modes for a 31-Hz Frequency

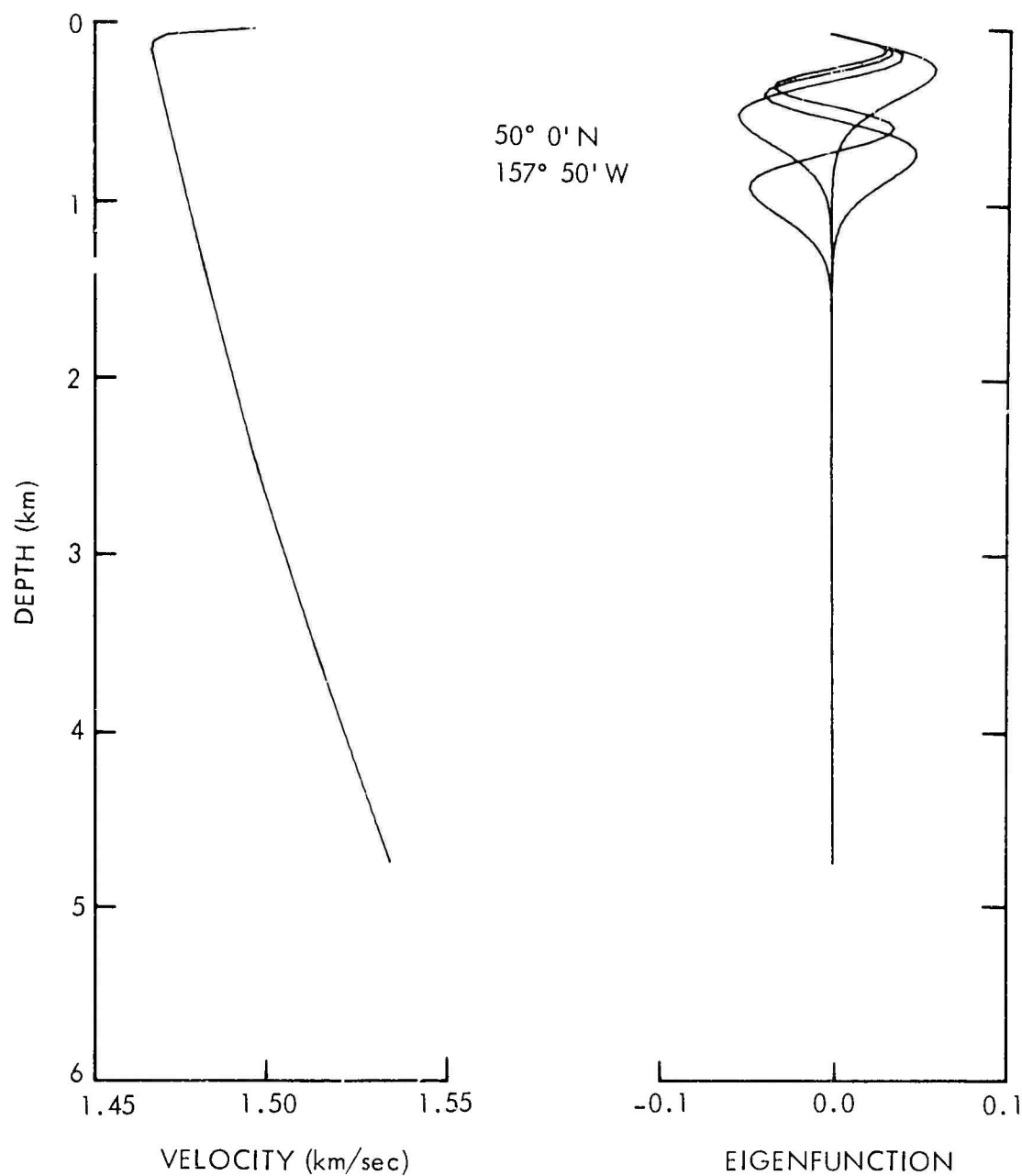


Figure 15. Sound Speed-Depth Profile at 50° 0'N, 157° 50'W and the Corresponding First Four Modes for a 31-Hz Frequency

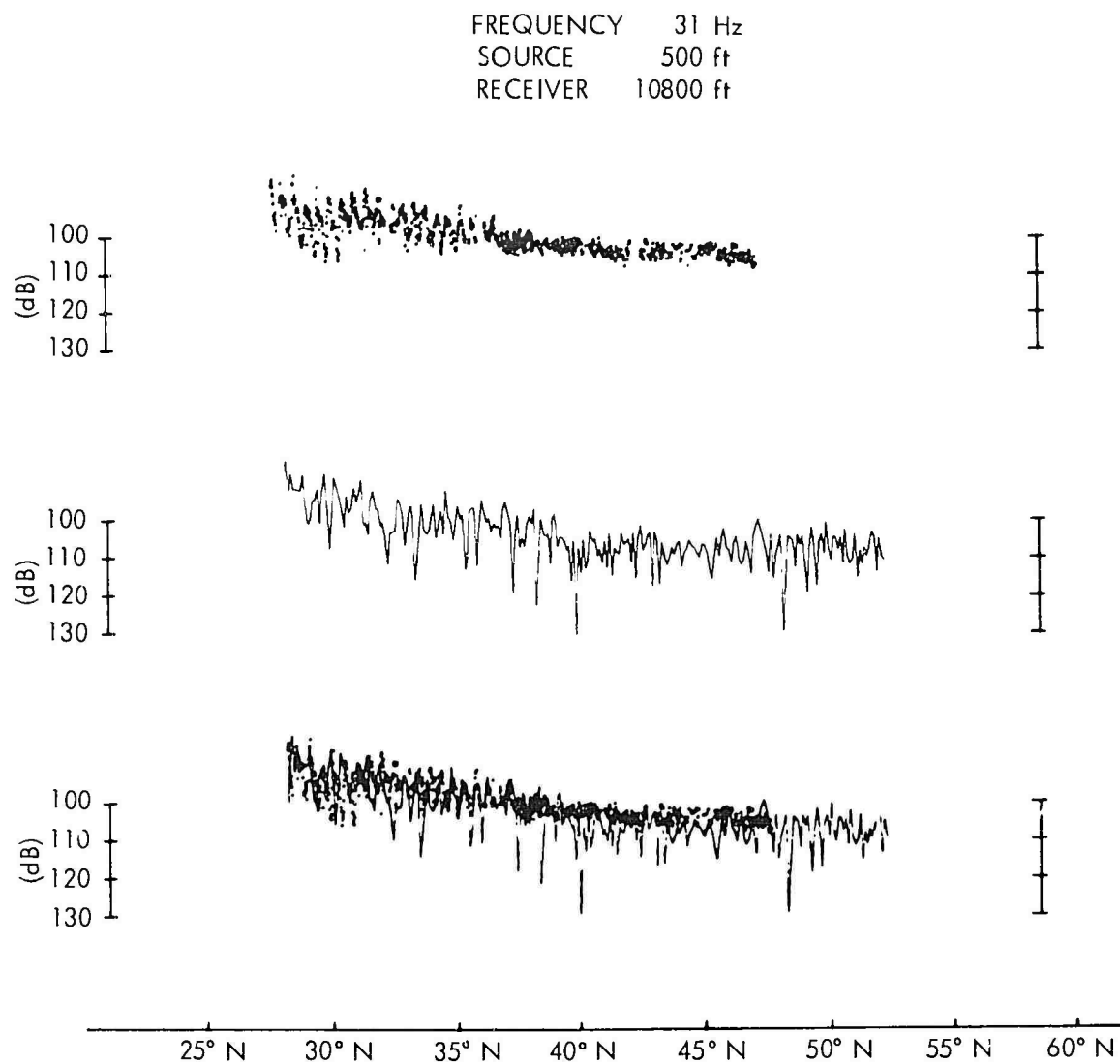


Figure 16. Propagation Loss versus Range for a 10,800-ft Receiver Depth,  
a 500-ft Source Depth, and a 31-Hz Frequency



## SUMMARY

Contrary to popular belief, ray theory is an accurate and efficient means of investigating low frequency acoustic propagation in the ocean. Of course, in this report ray theory has not been used in its classical sense.

Several illustrative examples proved that it is possible to design a single propagation model that agrees with analytic solutions and measured data, as well as other computer programs. This effort is more difficult than one may realize, for once a computer program is tuned to the actual environmental conditions of a real ocean, it may be impossible to input data for which analytic solutions are known. The apparently simple task of comparing programs is in reality even more difficult than a comparison with analytic solutions. First, one must have access to the programs being compared. Second, the programs must treat the input data similarly. Finally, the programs must treat the output data similarly. For example, how is one to compare coherent phase propagation loss predictions with those of a random phase program?

Although all the computer models discussed above have been designed within the last few years, the theories upon which they are based are much older. Therefore, it is felt that improved computing facilities rather than improved acoustic theories have been responsible for improved prediction capabilities.

The future of ray theory may prove quite different. Application to unstratified media, random media, etc. is the next logical step, but these theories need more development before they can be implemented into practical prediction models.

## REFERENCES

1. C. B. Officer, Introduction to the Theory of Sound Transmission, McGraw-Hill Book Company, New York, 1958.
2. M. A. Pedersen, "Acoustic Intensity Anomalies Introduced by Constant Velocity Gradients," Journal of the Acoustical Society of America, vol. 33, no. 4, April 1961, pp. 465-474.
3. C. B. Moler and L. P. Solomon, "Use of Splines and Numerical Integration in Geometrical Acoustics," Journal of the Acoustical Society of America, vol. 48, no. 3, September 1970, pp. 739-744.
4. A. K. Cline, "Scalar- and Planar-Valued Curve Fitting Using Splines Under Tension," Communications of the ACM, vol. 17, no. 4, April 1974, pp. 218-220.
5. M. A. Pedersen and D. F. Gordon, "Normal-Mode and Ray Theory Applied to Underwater Acoustic Conditions of Extreme Downward Refraction," Journal of the Acoustical Society of America, vol. 51, no. 1, January 1974, pp. 323-368.
6. L. Brekhovskikh, Waves in Layered Media, Academic Press, New York, 1960.
7. D. Ludwig, "Uniform Asymptotic Expansions at a Caustic," Communications on Pure and Applied Mathematics, vol. 19, no. 1, 1966, pp. 215-250.
8. B. Van der Pol and H. Bremmer, "The Diffraction of Electromagnetic Waves from an Electrical Point Source Round a Finitely Conducting Sphere, with Application to Radio Telegraphy and the Theory of the Rainbow," Philosophical Magazine, vol. 24, pt. 1, July 1937, pp. 141-176, and pt. 2, November 1937, pp. 825-864.
9. G. A. Leibiger and D. Lee, "Application of Normal Mode Theory to Convergence Zone Propagation," Vitro Laboratory Research Memorandum VL-8512-12-0, Vitro Laboratories, West Orange, New Jersey, 30 November 1968.
10. E. L. Murphy, "Modified Ray Theory for the Two-Turning-Point Problem," Journal of the Acoustical Society of America, vol. 47, no. 3, March 1970, pp. 899-908.
11. F. R. DiNapoli, Fast Field Program for Multilayered Media, NUSC Technical Report 4103, 26 August 1971.
12. Acoustic Environmental Support Detachment, "Fast Asymptotic Coherent Transmission (FACT) Model," Office of Naval Research, 1 April 1973.

13. G. A. Leibiger and D. Lee (This program has not yet been documented. See reference 9 for an earlier version.)
14. H. Weinberg, Navy Interim Surface Ship Model (NISSM) II, NUSC Technical Report 4527, 14 November 1973.
15. H. Weinberg and R. Burridge, "Horizontal Ray Theory for Ocean Acoustics," Journal of the Acoustical Society of America, vol. 55, no. 1, January 1974, pp. 63-79.
16. A. D. Pierce, "Extension of the Method of Normal Modes to Sound Propagation in an Almost-Stratified Medium," Journal of the Acoustical Society of America, vol. 37, no. 1, January 1965, pp. 19-27.